ACS OMEGA

Article

Cite This: ACS Omega 2018, 3, 1213−1219

Nondestructive Approach for Additive Nanomanufacturing of Metallic Nanostructures in the Air

Md Shah Alam[†] and Chenglong Zhao*[,†,‡]

[†]Department of Electro-Optics and Photonics and [‡]Department of Physics, University of Dayton, 300 College Park, Dayton, Ohio 45469, United States

Supporting Information

ABSTRACT: In this article, a mechanism for quick release and transfer of gold nanoparticles (GNPs) from a soft substrate to another substrate under laser illumination is investigated. The heating of GNPs on a soft substrate with a continuous-wave laser causes a rapid thermal expansion of the substrate, which can be used to selectively release and place GNPs onto another surface. In-plane and out-of-plane nanostructures are successfully fabricated using this method. This rapid release-and-place process can be used for additive nonmanufacturing of metallic nanostructures under ambient conditions, which paves a way for affordable nanomanufacturing and enables a wide variety of applications in nanophotonics, ultrasensitive sensing, and nonlinear plasmonics.

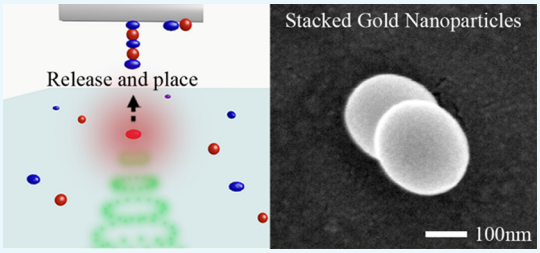

INTRODUCTION

Additive manufacturing at the macroscale has already been used for rapid prototyping. However, such a rapid prototyping technique is yet to be developed for manufacturing at the nanoscale or nanomanufacturing.[1] The terms "nonmanufacturing" and "nanofabrication" are often used interchangeably,[2] although Liddle and Gallatin have distinguished these two terms by using the criterion of economic viability.[3] There are a large number of nanomanufacturing approaches available, but only a few are suitable for additive nanomanufacturing. Manufacturing of metallic nanostructures with small gaps, such as nanodimers, is practically important for many applications including surface-enhanced Raman spectroscopy[4,5] and nonlinear plasmonics.[6,7]

Colloidal nanoparticles have been used as building blocks for this purpose because of the ease of massive production with well-designed size, shape, and superior crystal.[8−12] For example, gold nanodimers can be formed by linking individual nanoparticles with deoxyribonucleic acid (DNA).[13,14] The size of the gap in these nanodimers can be precisely controlled by the length of the DNA trains. However, this process is still stochastic and challenging to achieve high yield. Optical printing based on optical forces is another method that can be potentially used for additive nanomanufacturing. In this method, nanoparticles in colloidal solution are first brought close to a surface and then printed on the surface with a highly focused laser beam because of the strong optical force.[15−18] Isolated nanoparticles, such as spherical gold nanoparticles (GNPs),[17,19,20] gold nanodisks,[21] gold bipyramids,[22] and aligned gold nanorods,[15] have been successfully manufactured using this method. However, it is still challenging to manufacture nanostructures with small gaps using this method because of the thermophoretic repulsive force,[15,21,23−25] which limits the minimum size of the gap that can be formed between two adjacent nanoparticles. Several alternative approaches have been proposed to overcome this limitation such as printing nanoparticles on a thermo-responsive flexible polymer film,[25] selective printing of different types of metallic nanoparticles with lasers of different wavelengths,[23] and printing on a substrate with high thermal conductivity.[21] However, these methods are typically applicable in aqueous solution and are not suitable for certain applications where surface contamination has to be avoided.

In this article, we demonstrate a quick release-and-place approach that can be used to selectively release GNPs from a soft substrate and transfer them additively to any other substrates. The whole process is accomplished in the air, and there is no requirement for vacuum or high voltage. Individual GNPs can be released in sequence and placed additively to form two-dimensional (2D) and three-dimensional (3D) nanostructures without worrying about the thermophoretic force that limits the minimum gap between adjacent nanoparticles as that exists in the optical printing method.

RESULTS AND DISCUSSION

Figure 1a schematically shows the experimental setup of the release-and-place approach, which is based on the heating of GNPs and rapid thermal expansion of a soft substrate. A continuous-wave (CW) laser with a wavelength of 1064 nm serves as the heating laser. The laser beam is first expanded with two lenses (L1 and L2) and then reflected by a dichroic mirror (DM). Finally, it is focused on the sample with an oil-

Received: December 1, 2017
Accepted: January 18, 2018
Published: January 30, 2018

DOI: 10.1021/acsomega.7b01907
ACS Omega 2018, 3, 1213−1219

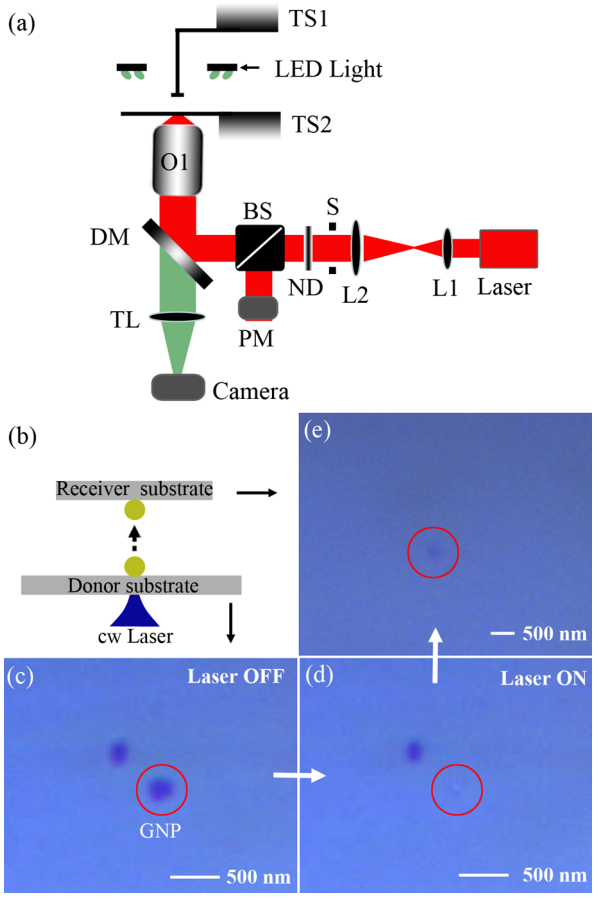

Figure 1. (a) Layout of the experimental setup. L: lens; TL: tube lens; DM: dichroic mirror; BS: beam splitter; O1: objective lens; PM: power meter; TS: translation stage; ND: variable neutral density filter; S: shutter. (b) Schematic of the release-and-place process. (c) Optical image of GNPs on a donor substrate when the laser is off. (d) Targeted GNP released from the donor substrate when the laser is on. (e) Released GNP on the receiver substrate.

immersion objective lens (O1, NA = 1.25, 100×). The laser beam overfills the back aperture of O1 to make full use of the numerical aperture (NA). A fraction of the laser is picked up by a beam splitter (BS), and its power is measured with a power meter (PM). The laser power at the focus of O1 can be calibrated and calculated from the power measured on PM. A variable neutral density filter (ND) is used to adjust the laser power. A shutter (S) is used to switch the laser on and off. A plastic (polyvinyl chloride, PVC) coverslip (Ted Pella, Inc., 22 × 22 × 0.18 mm) is placed on a translation stage (TS2) for precise position control. Colloidal GNPs with a diameter of 200 nm from BBI solutions are diluted to 20 v/v % and then drop-cast on this PVC substrate. The GNP solution is then left naturally dried on the substrate.

A second substrate can be mounted on another translation stage (TS1) and suspended on top of the PVC substrate. A ring-shaped light-emitting diode light source is used for illumination, and the GNPs on the PVC substrate are imaged on a camera with the same objective lens O1 and a tube lens (TL). The location of the heating laser is marked on the camera for precise orientation of the targeted GNP. GNPs on the PVC substrate can be moved to the focus of the heating laser and released from the substrate, as schematically shown in Figure 1b. Because GNPs will be released from this substrate, we call them donor substrate (a PVC substrate in this case) in this article unless stated otherwise. Figure 1c shows the optical image of a GNP on the donor substrate when the laser is off. The red circle indicates the area to be illuminated with the heating laser. Once the heating laser is switched on, the GNP is immediately released from the donor substrate. Figure 1d shows the same optical image after the laser is turned on. The GNP in the red circle is released from the donor substrate and transferred to another substrate placed on top of it. The release of a GNP from the donor substrate is also shown in Supporting Video 1 in the Supporting Information. Because GNPs are transferred to the top substrate, we call them receiver substrate (a glass coverslip in this case) in this article unless stated otherwise. Figure 1e shows the optical image of the receiver substrate after the release-and-place process. The black dot in the red circle shows the GNP that is placed on the receiver substrate, whose optical image is blurred because of the spherical aberration of O1 when imaging through the air. The experiment has been repeated by replacing the GNP with a polymer bead (diameter of 2.1 μm); however, the polymer bead cannot be released from the substrate as shown in the Supporting Information (Figure S1). This control experiment manifests the importance of effective light absorption and heating of particles for this method.

The donor substrate needs to be a soft substrate for a successful release-and-place process. However, there is no limitation on the type of the receiver substrate used in this method. When a GNP is illuminated with a CW laser, it serves as an efficient nanoheating source and converts the laser energy into heat.[26−28] The heating of the GNP induces a rapid thermal expansion of the donor substrate beneath the GNP, which gives the GNP an upward momentum and lifts the GNP off the donor substrate. To verify the aforementioned mechanism and exclude other possible forces such as optical force in this process, the following control experiments are conducted:

(1) Hard substrate: Figure 2a schematically shows the experimental configuration. Colloidal GNP solution is

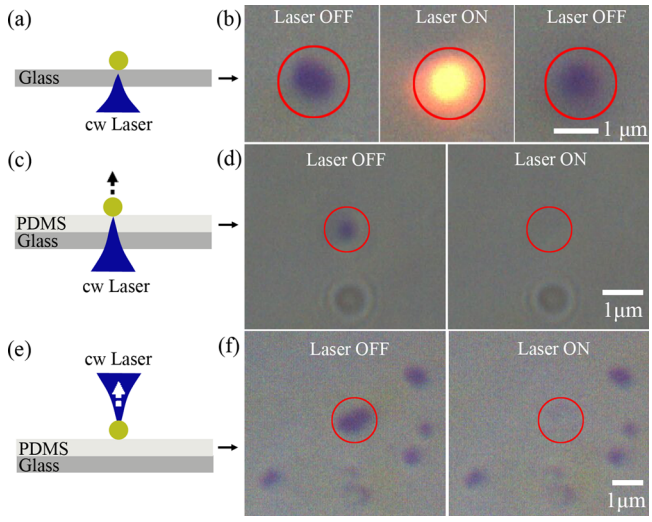

Figure 2. (a,b) GNPs cannot be released from a hard substrate. (c,d) GNPs can be released from a PDMS film on a hard substrate. (e,f) GNPs can be released from a flexible substrate in a direction opposite to the direction of optical radiation force. The white dashed arrow in (e) shows the moving direction of the GNPs that are released from the surface.

DOI: 10.1021/acsomega.7b01907
ACS Omega 2018, 3, 1213−1219

dried on a glass substrate (Ted Pella, Inc., micro cover glasses, 22 × 22 mm × 0.16−0.19 mm thick) following the same procedure as described earlier. Figure 2b shows the optical image of a cluster of GNPs on the glass substrate when the laser is off (left panel), on (middle panel), and off again (right panel). The visible light emission from the GNPs shown in the middle panel of Figure 2b may originate from the thermal radiation of the GNPs. However, the GNPs are still on the substrate after laser heating (refer to Supporting Video 2, Supporting Information for more details on this process). This experiment clearly shows that GNPs cannot be released from a hard substrate.

(2) Soft film on a hard substrate: to verify that a soft substrate plays the key role in this process, the same experiment is conducted on a soft film on a hard substrate. A polydimethylsiloxane (PDMS) film with a thickness of 100 μm is spin-coated on a glass coverslip. A PDMS solution is prepared by mixing Sylgard 184 silicone elastomer base and curing agent (Dow Corning Corporation, Michigan, USA).[29] The colloidal solution of the GNPs is then drop-cast on the PDMS film and naturally dried. Figure 2c,d shows that a GNP can be released from the PDMS film (refer to Supporting Video 3, Supporting Information for more details on this process).

(3) Exclude optical radiation force: the optical radiation force on the GNP that originates from the light momentum transfer may also play an important role in the release process. To justify the effect of this force on the release process, the same soft film on a hard substrate is used for this experiment. However, the laser is focused on a cluster of GNPs in the opposite direction, as schematically shown in Figure 2e. If the optical radiation force dominates in this process, the GNPs would be pushed in the direction of the laser, that is, into the PDMS film. However, the GNPs are still released from the PDMS film in a direction that is opposite to the incident laser direction, as shown in Figure 2f (refer to Supporting Video 4, Supporting Information for more details on this process). This control experiment clearly shows that the optical force does not dominate in the release process.

To further understand this release process, we simulated the thermal expansion of a PVC substrate because of the heating of a GNP by using a finite element method (COMSOL Multiphysics). The heat source (Q) comes from the heating of a GNP (diameter 200 nm) with a CW laser beam (1064 nm). The value of the heat source is calculated as

$$Q = \frac{\sigma_{abs} \times I}{V_{GNP}} \quad (1)$$

where σ_{abs}, I, and V_{GNP} are the absorption cross section, laser intensity, and the volume of the GNP, respectively. The absorption cross section σ_{abs} of a 200 nm GNP (surrounded by air on a PVC substrate) for a 1064 nm laser is calculated by using the Mie theory with an effective refractive index of $n_{eff} = 0.23n_{sub} + 0.77n_{air}$ following ref 26. The refractive index of gold is taken from ref 30. The laser intensity used in the simulation is 45 mW/μm^2. The temperature-dependent material properties of a GNP and a plastic (PVC) substrate used in the simulation are obtained from refs 31−36.

Figure 3a shows the displacement of the GNP as well as the temperature distribution at 93 ns after laser illumination. The

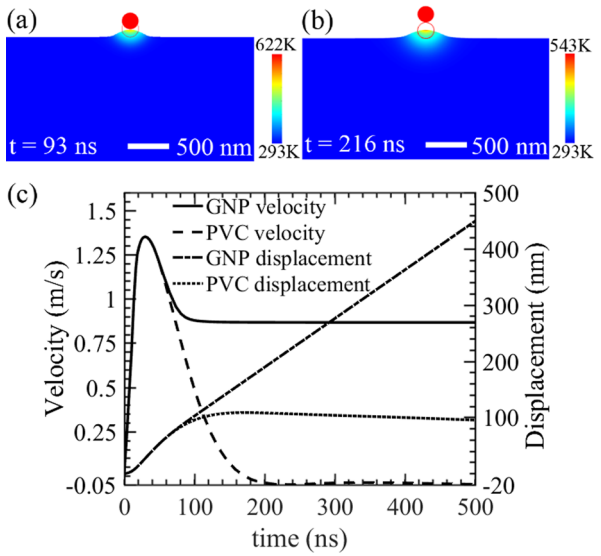

Figure 3. Simulation of the release process. (a,b) Displacement and temperature distribution of a GNP on a PVC substrate at 93 and 216 ns after laser illumination, respectively. The red circle shows the original position of the GNP on the substrate before laser illumination. (c) Displacement and velocity of the GNP and the substrate's surface under laser illumination.

substrate's surface underneath the GNP expands and pushes the GNP upward in the same direction. The GNP gains momentum because of the expansion of the plastic substrate but still remains in contact with the substrate because of van der Waals force. The expansion of the PVC substrate continues until the GNP gains enough momentum to overcome the van der Waals force between the GNP and the substrate before it is released from the substrate. Figure 3b shows the release of the GNP from the substrate with a displacement of 96 nm from the substrate's surface at 216 ns after laser illumination. Notice that the temperature of the GNP decreases because of the displacement from the laser focus (Supporting Information, Supporting Video 5). Figure 3c shows the velocity and displacement of the GNP as well as the substrate surface. The velocity of the GNP remains the same with the substrate surface and increases at the beginning of the release process because of the increased thermal expansion rate of the substrate. The expanding substrate surface pushes the GNP upward with the same velocity and is still in contact with the GNP. The velocity of the substrate's surface reaches a maximum of 1.35 m/s at 30 ns and begins to decrease because of the reduced expansion rate of the substrate. A detailed explanation of the particle release process can be found in the Supporting Information (Figure S2). If the PVC substrate is replaced by a PDMS substrate, it undergoes the same process. The thermal expansion of a PDMS substrate due to the heating of a GNP is shown in the Supporting Information (Figure S3).

Here, the gravitational force of the GNP has been ignored because it is 7 orders of magnitude smaller than the van der Waals force. The van der Waals force is calculated as follows[37]

$$F = -\frac{\sqrt{A_G \times A_{sub}}\, r}{6D^2} \quad (2)$$

DOI: 10.1021/acsomega.7b01907
ACS Omega 2018, 3, 1213−1219

where A_G and A_{sub} are Hamaker constants of the GNP and the PVC substrate, respectively.[38] r is the radius of the GNP. D is the separation between the GNP and the substrate. The van der Waals force decreases dramatically as the gap between the GNP and the substrate increases, as shown in Figure 4a. Because of

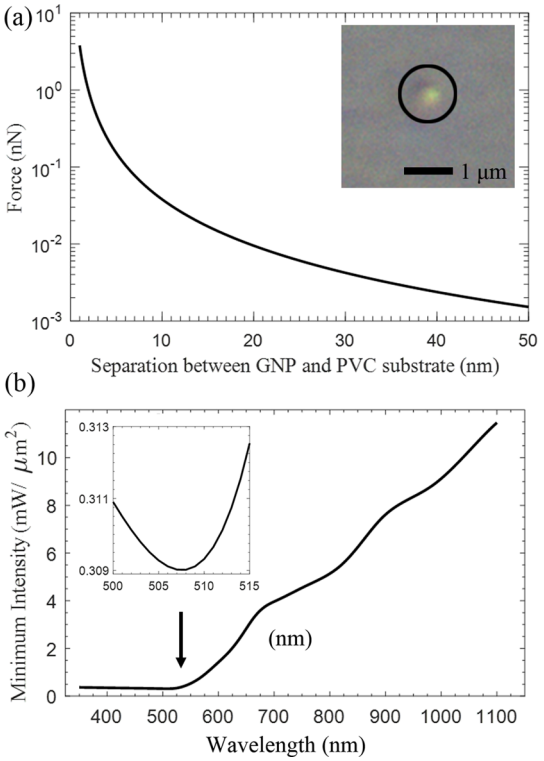

Figure 4. (a) van der Waals force between a GNP and a PVC substrate. The inset shows the optical image of the area from where the GNP is released. (b) Minimum laser intensity that is required to release a 200 nm GNP from a PVC substrate for lasers of different wavelengths. The inset shows the detail of the curve as marked by the black arrow.

the surface roughness of the plastic substrate, we consider an effective gap of 2 nm between the GNP and the PVC substrate, which results in a van der Waals force of 0.95 nN similar to that used in the simulation.

It should be noted that the simulation demonstrated here is a simplified model to illustrate the working principle of the release process. In reality, the substrate's surface beneath the GNP can be melted because of the high temperature of the GNP. The inset in Figure 4a shows the optical image of the PVC substrate after a GNP is released. The area beneath the GNP is marked in the black circle, which shows the surface morphology change once a GNP is released. In this case, not only the van der Waals force but also the surface tension between the GNP and the melted surface contribute in the release process. The surface tension between a GNP and a liquid surface can be approximately represented by the following equation[39]

$$F = 4\pi r\gamma \tag{3}$$

where r is the radius of the particle and γ is the surface tension of the liquid. However, in the case of the interaction between a spherical particle and a liquid droplet, this force strongly depends on the ratio of the particle to the droplet size $\nu = r/R$, where r and R are the radii of the particle and the droplet, respectively. Therefore, the analytical expression of the surface tension can be given by the following equation in the limit of small ν[40]

$$F = \mu\pi r\gamma \tag{4}$$

where μ is a parameter which depends on ν and the contact angle between the particle and the liquid droplet.[40] Force increases with the increase of contact angle but decreases with the increases of the ratio of particle to droplet size (ν). In our experiment, we can approximately take the melted surface as a liquid droplet with a radius of 215 nm (ν = 0.46) as measured from the inset of Figure 4a. Therefore, assuming the contact angle $\theta = 90°$, the approximate value of surface tension can be found as 6 nN, which is larger than that of the van der Waals force. Therefore, the dominant force at the moment of the GNP release will be the surface tension.

Various capping agents (surfactants, ligands, polymers, etc.) are typically used to prepare and stabilize GNPs in the liquid phase and can also be used to modify the interaction of the GNPs with their environment. The significance of these capping agents in the self-assembly of nanoparticles has been studied in different literature.[41−44] Moreover, surface wettability also affects the transfer of nanoparticles from one substrate to another.[45] Therefore, the possible role of the capping agents as well as the wettability of the substrate needs to be taken into account in the release process. The GNPs used in our experiment are citrate-stabilized with a negative surface charge in the solution; however, the GNP colloidal solution is completely dried on the substrate before the release process. Therefore, the surface charge of the GNPs differs from its native aqueous environment and is not characterized in our experiment. Basically, the surface charges of the GNPs will contribute an additional electrostatic force being attractive (with a surface charge of opposite sign to the substrate) or repulsive (with a surface charge of the same sign to the substrate) in the release-and-place process. In addition, the water molecules in humid air can enter the gaps between the GNPs and the substrate and absorbed on a sufficiently hydrophilic surface, which induces a capillary force on the GNP.[46−48] However, the relative importance of this capillary force strongly depends on the relative humidity (RH) of the air.[49,50] The capillary force is generally negligible when the RH is below 50%.[51] In our experiment, the RH is kept at 36%. Therefore, we neglected the capillary force in our analysis.

In our experimental conditions, a GNP can be released from the donor (PVC) substrate with a minimum laser intensity of 11 mW/μm^2. It should be noted that the minimum laser intensity that is required to release a GNP can be further reduced by changing the laser wavelength. Figure 4b shows the calculated minimum laser intensity that is required to release a 200 nm GNP from a PVC substrate by using lasers of different wavelengths. In this calculation, the experimental minimum laser intensity of 11 mW/μm^2 for the 1064 nm laser is taken as a reference and we assume that a GNP will be released from the substrate by the lasers of different wavelengths when the absorbed power ($P = \sigma_{abs}I$) by the GNP is similar to that of the reference condition. A laser with a shorter wavelength is preferred to efficiently heat the GNP and release it from the substrate. A GNP can be released from a PVC substrate with a minimum of 0.31 mW/μm^2 with a 508 nm laser, as shown in the inset of Figure 4b.

This rapid release process allows us to selectively and additively transfer GNPs to other substrates to form 2D or even

DOI: 10.1021/acsomega.7b01907
ACS Omega 2018, 3, 1213−1219

3D nanostructures. Here, we demonstrate the additive nanomanufacturing of gold nanodimers and nanotrimers on the core area of a fiber tip as a proof of concept. In this experiment, a PVC substrate with a thickness of 0.18 mm is used as the donor substrate. A single-mode fiber (Newport, core diameter: 3.4 μm, cladding diameter: 125 μm) that is placed on top of the donor substrate is used as the receiver substrate, as schematically shown in Figure 5a. The receiver

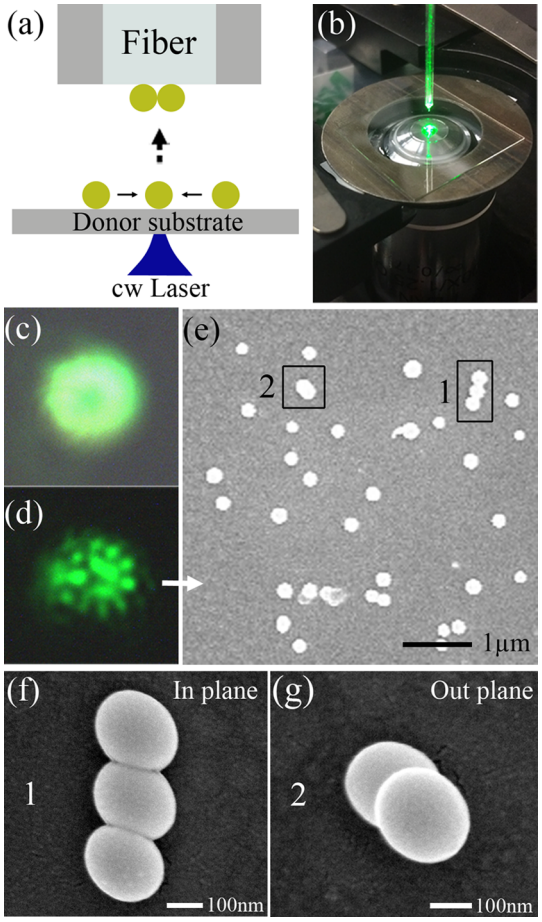

Figure 5. (a) Schematic of the experimental setup for additive nanomanufacturing on the fiber tip. (b) Part of the experimental setup. (c) Optical image of the fiber tip. (d) Optical image of the fiber tip after transferring several GNPs on it. (e) SEM image of the fiber tip. (f) SEM image of an in-plane gold nanotrimer on the fiber tip. (g) SEM image of an out-plane gold nanodimer on the fiber tip.

substrate shown in Figure 1a is replaced with this optical fiber. The optical fiber is mounted on the translation stage TS1 and is brought close to the donor substrate. Figure 5b shows a part of the experimental setup (an objective lens, a translational stage TS2, a donor substrate, a fiber holder, and a fiber tip) used for this experiment.

The light from a green laser is coupled into the optical fiber and the output light from the fiber tip is imaged on the same camera as shown in Figure 1a, where the position of the heating laser is marked. Figure 5c shows the optical image of the fiber tip with the core area clearly visible, which allows us to precisely align the fiber tip to the GNPs that need to be released from the substrate. The GNPs are moved in the heating laser one by one by moving the translation stage TS2. Once a GNP is released from the PVC substrate and placed on the fiber tip, the next GNP is moved in the heating laser and placed additively on the fiber tip. This process continues till the desired number of GNPs is fabricated on the core area of the fiber tip. Figure 5d shows the optical image of the same fiber tip after several GNPs are additively placed on the fiber. The scattering light from the GNPs is clearly seen in the image. Figure 5e shows the corresponding scanning electron microscopy (SEM) image of the optical fiber after the release-and-place process. Because of the surface roughness of the PVC substrate, each GNP in the release-and-place process does not always follow the same trajectory, but some GNPs do follow similar trajectories, which form closely packed gold nanodimers and nanotrimers as shown in the two black boxes (marked as 1 and 2 in Figure 5e). The corresponding SEM images at a higher magnification are shown in Figure 5f,g, respectively. Each GNP is fabricated on the fiber tip that is away from the focus of the heating laser; therefore, there is no need to worry about the thermophoretic repulsive force that exists in the optical printing methods.[15,21,23−25] This means that there is no limitation on the smallest gap that can be formed between two adjacent GNPs. Figure 5f shows the SEM image of an in-plane gold nanotrimer consisting of three touching GNPs. Here, in-plane means the nanotrimer lies in a plane parallel to the fiber surface. Figure 5g shows the SEM image of an out-plane nanodimer consisting of two stacked GNPs. Here, out-plane means the nanodimer lies in a direction that is normal to the fiber surface.

In spite of the stochastic nature of the additive manufacturing method demonstrated in this article, its low-cost and easy-to-implement properties introduce a new way for affordable and rapid prototyping. The fabrication accuracy of this method can be potentially improved by the following three steps, which will be investigated in our future works: (1) improve the flatness of the donor substrate by spin-coating a polymer (such as PDMS) on an ultraflat substrate; (2) reduce and optimize the distance between the receiver substrate and the donor substrate; and (3) apply an electric field between the donor and the receiver substrate.

CONCLUSIONS

In conclusion, an affordable additive nanomanufacturing method is investigated in this article. Because of the heating of the GNP and the rapid surface expansion of the soft donor substrate, GNPs can be additively transferred to any receiver substrate. There is no limitation on the type of the receiver substrate for this method. In addition, no expensive pulsed laser is required for this approach. The use of a low-cost CW laser makes affordable and rapid prototyping of closely packed nanostructures possible. It should be noted that the method demonstrated in this article is different from direct laser ablation,[52−55] where expensive pulsed lasers are used to ablate the materials disruptively and the fabricated nanostructures are limited to spherical shapes only. The method demonstrated in this article has no damage on the nanostructures to be released from the substrate. Nanostructures with any desired shapes can be selectively and nondestructively released from a donor substrate and additively transferred to another substrate. Therefore, this method paves a potential new way of manufacturing nanostructures with small gaps for applications in ultrafast sensing and nonlinear optics.

DOI: 10.1021/acsomega.7b01907
ACS Omega 2018, 3, 1213−1219

■ ASSOCIATED CONTENT

Supporting Information

The Supporting Information is available free of charge on the ACS Publications website at DOI: 10.1021/acsomega.7b01907.

Experimental result of laser illumination of a polymer bead; schematic of force analysis of the release-and-place process; and simulation of a GNP released from a PDMS substrate (PDF)

Release of a GNP from the soft donor substrate (AVI)

GNPs still on the hard substrate after laser heating (AVI)

Release of a GNP from the PDMS film (AVI)

Release of GNPs from the PDMS film in a direction that is opposite to the incident laser direction (AVI)

Decrease of temperature in the GNP because of the displacement from the laser focus (AVI)

■ AUTHOR INFORMATION

Corresponding Author

*E-mail: czhao1@udayton.edu (C.Z.).

ORCID

Md Shah Alam: 0000-0003-3694-0267

Chenglong Zhao: 0000-0003-2831-1671

Notes

The authors declare no competing financial interest.

■ ACKNOWLEDGMENTS

The authors acknowledge financial support from the open access fund and the summer research fellowship at the University of Dayton.

■ REFERENCES

(1) Engstrom, D. S.; Porter, B.; Pacios, M.; Bhaskaran, H. Additive Nanomanufacturing – A Review. *J. Mater. Res.* **2014**, *29*, 1792−1816.

(2) Hirt, L.; Reiser, A.; Spolenak, R.; Zambelli, T. Additive Manufacturing of Metal Structures at the Micrometer Scale. *Adv. Mater.* **2017**, *29*, 1604211.

(3) Liddle, J. A.; Gallatin, G. M. Nanomanufacturing: A Perspective. *ACS Nano* **2016**, *10*, 2995−3014.

(4) Schlücker, S. Surface-Enhanced Raman Spectroscopy: Concepts and Chemical Applications. *Angew. Chem., Int. Ed.* **2014**, *53*, 4756−4795.

(5) Lim, D.-K.; Jeon, K.-S.; Hwang, J.-H.; Kim, H.; Kwon, S.; Suh, Y. D.; Nam, J.-M. Highly Uniform and Reproducible Surface-Enhanced Raman Scattering from DNA-Tailorable Nanoparticles with 1-Nm Interior Gap. *Nat. Nanotechnol.* **2011**, *6*, 452−460.

(6) Kauranen, M.; Zayats, A. V. Nonlinear Plasmonics. *Nat. Photonics* **2012**, *6*, 737−748.

(7) Butet, J.; Brevet, P.-F.; Martin, O. J. F. Optical Second Harmonic Generation in Plasmonic Nanostructures: From Fundamental Principles to Advanced Applications. *ACS Nano* **2015**, *9*, 10545−10562.

(8) Daniel, M.-C.; Astruc, D. Gold Nanoparticles: Assembly, Supramolecular Chemistry, Quantum-Size-Related Properties, and Applications toward Biology, Catalysis, and Nanotechnology. *Chem. Rev.* **2004**, *104*, 293−346.

(9) Murphy, C. J.; Sau, T. K.; Gole, A. M.; Orendorff, C. J.; Gao, J.; Gou, L.; Hunyadi, S. E.; Li, T. Anisotropic Metal Nanoparticles: Synthesis, Assembly, and Optical Applications. *J. Phys. Chem. B* **2005**, *109*, 13857−13870.

(10) Chaudhuri, R. G.; Paria, S. Core/Shell Nanoparticles: Classes, Properties, Synthesis Mechanisms, Characterization, and Applications. *Chem. Rev.* **2012**, *112*, 2373−2433.

(11) Sun, Y.; Xia, Y. Shape-Controlled Synthesis of Gold and Silver Nanoparticles. *Science* **2002**, *298*, 2176−2179.

(12) Xia, Y.; Xiong, Y.; Lim, B.; Skrabalak, S. E. Shape-Controlled Synthesis of Metal Nanocrystals: Simple Chemistry Meets Complex Physics? *Angew. Chem., Int. Ed.* **2009**, *48*, 60−103.

(13) Lan, X.; Chen, Z.; Lu, X.; Dai, G.; Ni, W.; Wang, Q. DNA-Directed Gold Nanodimers with Tailored Ensemble Surface-Enhanced Raman Scattering Properties. *ACS Appl. Mater. Interfaces* **2013**, *5*, 10423−10427.

(14) Göeken, K. L.; Schasfoort, R. B. M.; Subramaniam, V.; Gill, R. Spermine Induced Reversible Collapse of Deoxyribonucleic Acid-Bridged Nanoparticle-Based Assemblies. *Nano Res.* **2017**, *11*, 383−396.

(15) Do, J.; Fedoruk, M.; Jäckel, F.; Feldmann, J. Two-Color Laser Printing of Individual Gold Nanorods. *Nano Lett.* **2013**, *13*, 4164−4168.

(16) Violi, I. L.; Gargiulo, J.; von Bilderling, C.; Cortés, E.; Stefani, F. D. Light-Induced Polarization-Directed Growth of Optically Printed Gold Nanoparticles. *Nano Lett.* **2016**, *16*, 6529−6533.

(17) Urban, A. S.; Lutich, A. A.; Stefani, F. D.; Feldmann, J. Laser Printing Single Gold Nanoparticles. *Nano Lett.* **2010**, *10*, 4794−4798.

(18) Nedev, S.; Urban, A. S.; Lutich, A. A.; Feldmann, J. Optical Force Stamping Lithography. *Nano Lett.* **2011**, *11*, 5066−5070.

(19) Hoogenboom, J. P.; Vossen, D. L. J.; Faivre-Moskalenko, C.; Dogterom, M.; van Blaaderen, A. Patterning Surfaces with Colloidal Particles Using Optical Tweezers. *Appl. Phys. Lett.* **2002**, *80*, 4828−4830.

(20) Guffey, M. J.; Scherer, N. F. All-Optical Patterning of Au Nanoparticles on Surfaces Using Optical Traps. *Nano Lett.* **2010**, *10*, 4302−4308.

(21) Gargiulo, J.; Brick, T.; Violi, I. L.; Herrera, F. C.; Shibanuma, T.; Albella, P.; Requejo, F. G.; Cortés, E.; Maier, S. A.; Stefani, F. D. Understanding and Reducing Photothermal Forces for the Fabrication of Au Nanoparticle Dimers by Optical Printing. *Nano Lett.* **2017**, *17*, 5747−5755.

(22) Guffey, M. J.; Miller, R. L.; Gray, S. K.; Scherer, N. F. Plasmon-Driven Selective Deposition of Au Bipyramidal Nanoparticles. *Nano Lett.* **2011**, *11*, 4058−4066.

(23) Gargiulo, J.; Cerrota, S.; Cortés, E.; Violi, I. L.; Stefani, F. D. Connecting Metallic Nanoparticles by Optical Printing. *Nano Lett.* **2016**, *16*, 1224−1229.

(24) Bao, Y.; Yan, Z.; Scherer, N. F. Optical Printing of Electrodynamically Coupled Metallic Nanoparticle Arrays. *J. Phys. Chem. C* **2014**, *118*, 19315−19321.

(25) Urban, A. S.; Fedoruk, M.; Nedev, S.; Lutich, A.; Lohmueller, T.; Feldmann, J. Shrink-to-Fit Plasmonic Nanostructures. *Adv. Opt. Mater.* **2013**, *1*, 123−127.

(26) Setoura, K.; Okada, Y.; Werner, D.; Hashimoto, S. Observation of Nanoscale Cooling Effects by Substrates and the Surrounding Media for Single Gold Nanoparticles under CW-Laser Illumination. *ACS Nano* **2013**, *7*, 7874−7885.

(27) Setoura, K.; Ito, S.; Miyasaka, H. Stationary Bubble Formation and Marangoni Convection Induced by CW Laser Heating of a Single Gold Nanoparticle. *Nanoscale* **2017**, *9*, 719−730.

(28) Baffou, G.; Quidant, R.; García de Abajo, F. J. Nanoscale Control of Optical Heating in Complex Plasmonic Systems. *ACS Nano* **2010**, *4*, 709−716.

(29) Wang, S.; Kallur, A.; Goshu, A. Fabrication and Characterization of PDMS Thin Film. In *Proceedings of Organic Photonic Materials and Devices XIII*; SPIE, 2011; Vol. 7935, p 79350M.

(30) Johnson, P. B.; Christy, R. W. Optical Constants of the Noble Metals. *Phys. Rev. B: Solid State* **1972**, *6*, 4370−4379.

(31) Arblaster, J. W. Thermodynamic Properties of Gold. *J. Phase Equilibria Diffusion* **2016**, *37*, 229−245.

(32) Powell, R. W.; Ho, C. Y.; Liley, P. E. *Thermal Conductivity of Selected Materials*; U.S. Dept. of Commerce, National Bureau of Standards: Washington, DC, 1966; p 16.

(33) Nix, F. C.; MacNair, D. The Thermal Expansion of Pure Metals: Copper, Gold, Aluminum, Nickel, and Iron. *Phys. Rev.* **1941**, *60*, 597−605.

DOI: 10.1021/acsomega.7b01907
ACS Omega 2018, 3, 1213−1219

(34) Anderson, D. R. Thermal Conductivity of Polymers. *Chem. Rev.* **1966**, *66*, 677−690.
(35) Chang, S.-S. Heat Capacity and Thermodynamic Properties of Poly(Vinyl Chloride). *J. Res. Natl. Bur. Stand.* **1977**, *82*, 9−18.
(36) Povolo, F.; Schwartz, G.; Hermida, É. B. Stress Relaxation of PVC below the Yield Point. *J. Polym. Sci., Part B: Polym. Phys.* **1996**, *34*, 1257−1267.
(37) Guo, D.; Xie, G.; Luo, J. Mechanical Properties of Nanoparticles: Basics and Applications. *J. Phys. D Appl. Phys.* **2014**, *47*, 013001.
(38) Hamaker, H. C. The London—van Der Waals Attraction between Spherical Particles. *Physica* **1937**, *4*, 1058−1072.
(39) Ranade, M. B. Adhesion and Removal of Fine Particles on Surfaces. *Aerosol Sci. Technol.* **1987**, *7*, 161−176.
(40) Ettelaie, R.; Lishchuk, S. V. Detachment Force of Particles from Fluid Droplets. *Soft Matter* **2015**, *11*, 4251−4265.
(41) Sánchez-Iglesias, A.; Grzelczak, M.; Altantzis, T.; Goris, B.; Pérez-Juste, J.; Bals, S.; Van Tendeloo, G.; Donaldson, S. H.; Chmelka, B. F.; Israelachvili, J. N.; et al. Hydrophobic Interactions Modulate Self-Assembly of Nanoparticles. *ACS Nano* **2012**, *6*, 11059−11065.
(42) Fang, Y.; Guo, S.; Zhu, C.; Zhai, Y.; Wang, E. Self-Assembly of Cationic Polyelectrolyte-Functionalized Graphene Nanosheets and Gold Nanoparticles: A Two-Dimensional Heterostructure for Hydrogen Peroxide Sensing. *Langmuir* **2010**, *26*, 11277−11282.
(43) Hinterwirth, H.; Kappel, S.; Waitz, T.; Prohaska, T.; Lindner, W.; Lämmerhofer, M. Quantifying Thiol Ligand Density of Self-Assembled Monolayers on Gold Nanoparticles by Inductively Coupled Plasma−Mass Spectrometry. *ACS Nano* **2013**, *7*, 1129−1136.
(44) Pal, A.; Srivastava, A.; Bhattacharya, S. Role of Capping Ligands on the Nanoparticles in the Modulation of Properties of a Hybrid Matrix of Nanoparticles in a 2D Film and in a Supramolecular Organogel. *Chem.—Eur. J.* **2009**, *15*, 9169−9182.
(45) Hanske, C.; Müller, M. B.; Bieber, V.; Tebbe, M.; Jessl, S.; Wittemann, A.; Fery, A. The Role of Substrate Wettability in Nanoparticle Transfer from Wrinkled Elastomers: Fundamentals and Application toward Hierarchical Patterning. *Langmuir* **2012**, *28*, 16745−16750.
(46) Sedin, D. L.; Rowlen, K. L. Adhesion Forces Measured by Atomic Force Microscopy in Humid Air. *Anal. Chem.* **2000**, *72*, 2183−2189.
(47) de Lazzer, A.; Dreyer, M.; Rath, H. J. Particle−Surface Capillary Forces. *Langmuir* **1999**, *15*, 4551−4559.
(48) Xiao, X.; Qian, L. Investigation of Humidity-Dependent Capillary Force. *Langmuir* **2000**, *16*, 8153−8158.
(49) Henderson, M. The Interaction of Water with Solid Surfaces: Fundamental Aspects Revisited. *Surf. Sci. Rep.* **2002**, *46*, 1−308.
(50) Jones, R.; Pollock, H. M.; Cleaver, J. A. S.; Hodges, C. S. Adhesion Forces between Glass and Silicon Surfaces in Air Studied by AFM: Effects of Relative Humidity, Particle Size, Roughness, and Surface Treatment. *Langmuir* **2002**, *18*, 8045−8055.
(51) Mittal, K. L.; Jaiswal, R. *Particle Adhesion and Removal*; Wiley: New York, 2015; p 10.
(52) Evlyukhin, A. B.; Novikov, S. M.; Zywietz, U.; Eriksen, R. L.; Reinhardt, C.; Bozhevolnyi, S. I.; Chichkov, B. N. Demonstration of Magnetic Dipole Resonances of Dielectric Nanospheres in the Visible Region. *Nano Lett.* **2012**, *12*, 3749−3755.
(53) Zywietz, U.; Reinhardt, C.; Evlyukhin, A. B.; Birr, T.; Chichkov, B. N. Generation and Patterning of Si Nanoparticles by Femtosecond Laser Pulses. *Appl. Phys. A: Mater. Sci. Process.* **2014**, *114*, 45−50.
(54) Kuznetsov, A. I.; Evlyukhin, A. B.; Reinhardt, C.; Seidel, A.; Kiyan, R.; Cheng, W.; Ovsianikov, A.; Chichkov, B. N. Laser-Induced Transfer of Metallic Nanodroplets for Plasmonics and Metamaterial Applications. *J. Opt. Soc. Am. B* **2009**, *26*, B130−B138.
(55) Zywietz, U.; Evlyukhin, A. B.; Reinhardt, C.; Chichkov, B. N. Laser Printing of Silicon Nanoparticles with Resonant Optical Electric and Magnetic Responses. *Nat. Commun.* **2014**, *5*, 3402.

DOI: 10.1021/acsomega.7b01907
ACS Omega 2018, 3, 1213−1219